© 2014. Published by The Company of Biologists Ltd | Development (2014) 141, 3761-3771 doi:10.1242/dev.111005

RESEARCH ARTICLE

An Org-1–Tup transcriptional cascade reveals different types of alary muscles connecting internal organs in *Drosophila*

Hadi Boukhatmi[1,*,‡], Christoph Schaub[2,‡], Laetitia Bataillé[1,‡], Ingolf Reim[2], Jean-Louis Frendo[1], Manfred Frasch[2,§] and Alain Vincent[1,§]

ABSTRACT

The T-box transcription factor Tbx1 and the LIM-homeodomain transcription factor Islet1 are key components in regulatory circuits that generate myogenic and cardiogenic lineage diversity in chordates. We show here that Org-1 and Tup, the *Drosophila* orthologs of Tbx1 and Islet1, are co-expressed and required for formation of the heart-associated alary muscles (AMs) in the abdomen. The same holds true for lineage-related muscles in the thorax that have not been described previously, which we name thoracic alary-related muscles (TARMs). Lineage analyses identified the progenitor cell for each AM and TARM. Three-dimensional high-resolution analyses indicate that AMs and TARMs connect the exoskeleton to the aorta/heart and to different regions of the midgut, respectively, and surround-specific tracheal branches, pointing to an architectural role in the internal anatomy of the larva. Org-1 controls *tup* expression in the AM/TARM lineage by direct binding to two regulatory sites within an AM/TARM-specific cis-regulatory module, *tupAME*. The contributions of Org-1 and Tup to the specification of *Drosophila* AMs and TARMs provide new insights into the transcriptional control of *Drosophila* larval muscle diversification and highlight new parallels with gene regulatory networks involved in the specification of cardiopharyngeal mesodermal derivatives in chordates.

KEY WORDS: Tbx1, Org-1, Tup, Islet1, Alary muscle development, Transcriptional cascades, *Drosophila*

INTRODUCTION

The musculature of each animal species is composed of a stereotypical array of morphologically distinct muscles, which allows the precision and efficiency of body movements. Elucidating the mechanisms involved in conferring a specific morphology and function to each muscle remains a major challenge in myogenesis research. The somatic musculature of the *Drosophila* larva has for 20 years been a classical model with which to study this question. Each hemisegment of the larva shows a stereotypical arrangement of ~30 distinct body wall muscles, which attach to the exoskeleton at distinctive positions (Bate, 1993). Each body wall muscle is seeded by a founder cell (FC), which undergoes multiple rounds of fusion with fusion-competent myoblasts (FCMs) (Rushton et al., 1995). FCs are born from the asymmetric division of progenitor cells (PCs) specified at precise positions and times within the somatic mesoderm. Detailed characterization of a few somatic muscle lineages has established that muscle identity (specific shape, size, orientation) reflects the expression of specific muscle identity transcription factors (iTFs) in each FC that act in a combinatorial manner (Baylies et al., 1998; Frasch, 1999; de Joussineau et al., 2012; Enriquez et al., 2012).

In addition to body wall muscles, one alary muscle (AM) in each abdominal hemisegment connects the dorsal vessel, which is the functional equivalent of the heart, to the lateral epidermis. AMs were identified some years ago in *Drosophila* (Rizki, 1978), but have largely escaped attention. The name alary refers to a wing-like (aliform) shape. Sparse descriptions of AMs in adults of different insect species led to proposals of their role in maintaining the heart in its dorsal position or/and controlling ostia opening and heart beating (Dulcis and Levine, 2003; Glenn et al., 2010). A detailed ultrastructural study showed that AMs adhere to the pericardial cells via flexible extracellular matrix (ECM) fibers (Lehmacher et al., 2012). In the *Drosophila* embryo, seven pairs of AMs attach to the dorsal vessel in a segmental arrangement; four connect to the posterior heart proper in abdominal segments A4-A7 and three connect to the aorta in segments A1-A3. The absence of AMs in thoracic segments correlates with the anterior aorta ending at the T2/T3 boundary, and bending ventrally to form a funnel-shaped outflow tract that is anchored by the heart-anchoring cells and cardiac outflow muscles (Zmojdzian et al., 2008). We recently found that both Org-1 (Optomotor-blind-related-gene-1), which is the ortholog of the vertebrate T-box factor Tbx1, and Tailup (Tup), the ortholog of the LIM-homeodomain factor Islet1, are expressed in AMs, and we devised reporter genes that allow the embryonic development of these muscles to be followed (Schaub et al., 2012; Tao et al., 2007; Boukhatmi et al., 2012).

We report here on the transcriptional control of AM development and their attachment to the epidermis and heart tube. We show that AMs run internally and affixed to the main, dorsal branch of trachea and externally to the lateral branches. We also confirmed transient, sequential contacts between several AMs and the tip cells of the anterior Malpighian tubules (MTs), as recently reported by Weavers and Skaer (2013). Our lineage analyses further revealed the existence of alary-related muscles in the thorax, which connect the epidermis of thoracic segments T1 and T2 to precise positions of the midgut. We designate these previously unrecognized types of muscle as 'thoracic alary-related muscles' (TARMs). Thus, AMs and TARMs together connect the circulatory system and visceral organs to the exoskeleton of the larva, and buckle the trachea, suggesting that they play both anatomical and physiological roles during larval development.

AMs, as well as TARMs, are either missing or malformed in *org-1* and *tup* mutant embryos. Epistasis experiments and

[1]Université de Toulouse 3, Centre de Biologie du Développement, UMR 5547 CNRS and FRBT, 118 route de Narbonne, Toulouse F-31062, Cedex 09, France. [2]Friedrich-Alexander University of Erlangen-Nürnberg, Department of Biology, Division of Developmental Biology, Staudtstraβe 5, Erlangen 91058, Germany. *Present address: Department of Physiology, Development and Neuroscience, University of Cambridge, Downing Street, Cambridge CB2 3DY, UK. ‡These authors contributed equally to this work

§Authors for correspondence (manfred.frasch@fau.de; alain.vincent@univ-tlse3.fr)

Received 6 April 2014; Accepted 7 August 2014

Development (2014) 141, 3761-3771 doi:10.1242/dev.111005

mutational analysis of *tup* cis-regulatory modules (CRMs) show that *tup* expression is under direct control of Tup itself in body wall muscles and under the control of Org-1 in AMs. Vertebrate *Islet1* and *Tbx1* are major players in the genetic program that controls the fate of pharyngeal mesoderm progenitors, which give rise to several aspects of the heart and head musculature (Laugwitz et al., 2005; Moretti et al., 2006; Sambasivan et al., 2009; reviewed by Vincent and Buckingham, 2010). Future studies will be required to establish which ancestral regulatory interactions have been redirected to foster the emergence of insect AMs/TARMs and hypothetical functional equivalents in other phyla.

RESULTS

Org-1 and Tup are co-expressed in the abdominal alary muscles and in previously unrecorded alary-related muscles in the thorax

Org-1, the *Drosophila* ortholog of vertebrate Tbx1, is expressed in the three larval body wall muscles, namely LO1, VT1 and SBM, as well as in AM in abdominal segments, in addition to the visceral musculature (Schaub and Frasch, 2013). Tup is also expressed in AMs, in addition to the heart and the dorsal DA1, DA2, DO1 and DO2 muscles (Tao et al., 2007; Boukhatmi et al., 2012), dorsal ectoderm, amnioserosa and precursor cells of the pharynx (Thor and Thomas, 1997; Ashe et al., 2000). Expression of the *org-1-HN39-lacZ* (*org-1-lacZ*) reporter recapitulates *org-1* expression in the somatic musculature (Schaub et al., 2012), while both *IsletH-GFP* and *tupF4-GFP*, two overlapping reporter constructs, reproduce *tup* expression in AMs (Tao et al., 2007; Boukhatmi et al., 2012).

Staining embryos for *IsletH-GFP* and either Org-1 or *org-1-lacZ* [by β-galactosidase (β-gal)] expression confirmed that AMs are the only abdominal muscles expressing both Org-1 and Tup (Fig. 1A,B). It also revealed the existence of two multinucleated fibers straddling the thoracic T1-T3 and the T2-abdominal 1 (A1) segments, respectively (Fig. 1A-C). In addition to expressing both Org-1 and Tup, these transverse, multinucleated muscles, which do not attach to the heart, display a thin, very elongated shape similar to that of abdominal AMs (Fig. 1C). Henceforth, we refer to them as 'thoracic alary-related muscles' (TARMs). The discovery of TARMs prompted us to compare in detail the development and morphology of AMs and TARMs in *Drosophila* embryos.

AMs connect multiple organs

The morphological description of abdominal AMs has focused, so far, on their dorsal connection to pericardial cells that surround the cardiomyocytes in the abdominal segments (Rizki, 1978). Ultrastructural and immunocytochemistry studies performed in larvae and adults showed that AMs dorsally form delta-like extensions connecting to the ECM that surrounds pericardial cells and contains Pericardin (Prc) (Lehmacher et al., 2012). Three-dimensional reconstruction of embryos stained for *org-1-lacZ* and either Prc or β3-tubulin (β3-Tub), which stains all muscles, shows that the AMs run immediately anterior to abdominal segmental boundaries, with dorsal projections extending on either side of the boundary (Fig. 2A,F; supplementary material Fig. S1). The anterior dorsal extension of the AM in A1 connects to the posterior aspect of the lymph gland, which is the prospective posterior signaling center (Crozatier et al., 2004). Nomarski examination of embryos stained for *tup-moeGFP* reporter expression (see below) shows that the dorsal extensions of two adjacent AMs connect with one another (supplementary material Fig. S1).

To further describe AM morphology visualized with *org-1-lacZ*, we used additional markers. Staining for *stripe* (*sr*)>*GFP*, a marker of tendon cells, which mediate attachment of muscles to the exoskeleton (Frommer et al., 1996), showed that the ventral AM attachment site is positioned slightly dorsal to the SBM and ventral to the DO3 and LL1 epidermal attachment sites (Fig. 2A). Triple staining for β3-Tub, *tupAME-moeGFP* (see description below) and βPS integrin showed βPS accumulation both at the AM epidermal attachment site and at dorsal projections in contact with either the PSC or pericardial cells (supplementary material Fig. S2). Three-dimensional reconstruction of embryos stained for *sr>GFP* and Prc showed that AMs form an arc of a circle inside the body of the embryo (Fig. 2B,B′,F). Triple staining for β3-Tub, *org-1-lacZ* and 2A12 to visualize the tracheal network (Tiklova et al., 2013) indicated that AMs run internally to the dorsal, main tracheal branch, and externally to the ventral branch, suggesting an architectural role in pressing the dorsal branch against the body wall (Fig. 2C-C‴,F).

Finally, staining for Cut, a marker of MT cells, showed that the distal tip cell of anterior MTs makes specific, integrin-mediated transient contacts with specific AMs during the MT lengthening and bending process (supplementary material Fig. S2) (Weavers and Skaer, 2013). It first contacts the AM in A5 at the A5/A6 segmental boundary, then contacts the AM in A4 at the A3/A4 boundary, to finally anchor the MT to the AM in A3 at the A3/A4 boundary (Fig. 2D-D‴,F; data not shown). The dynamic sequence of MT tip cell/AM interactions has recently been described independently by Weavers and Skaer (2013). We further observed that the anterior MT tip cell is *org-1-lacZ* positive (Fig. 2E). Closer examination showed that the cell immediately following the tip cell is also slightly *org-1-lacZ* positive, suggesting

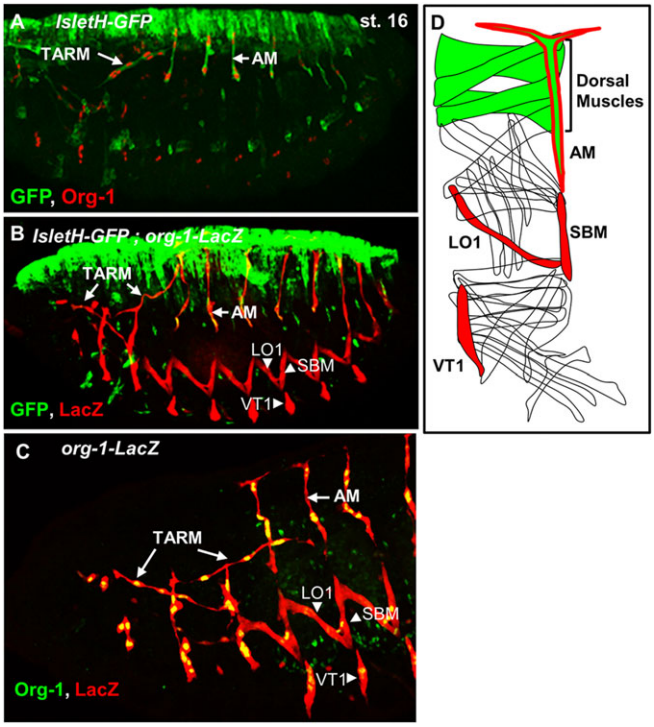

Fig. 1. Co-expression of Tup and Org-1 is specific to AMs and TARMs. (A-C) Stage 16 *IsletH-GFP* (A), *IsletH-GFP; org-1-lacZ* (B) and *org-1-lacZ* (C) embryos stained for GFP (green), Org-1 (A, red; C, green) and β-gal (B,C, red). AMs and TARMs co-express Org-1 and *tup* and *org-1* reporters (arrows). *IsletH-GFP* is also expressed in the dorsal epidermis and the heart, and *org-1-lacZ* in the SBM, LO1 and VT1 muscles (arrowheads in B,C). (C) Staining for *org-1-lacZ* (red) and Org-1 (green) shows that TARMs, like AMs, are multinucleated fibers. (D) Schematic of Org-1 and Tup expression in abdominal muscles. Unless otherwise indicated, lateral views of embryos are shown, with dorsal up and anterior left.

Development (2014) 141, 3761-3771 doi:10.1242/dev.111005

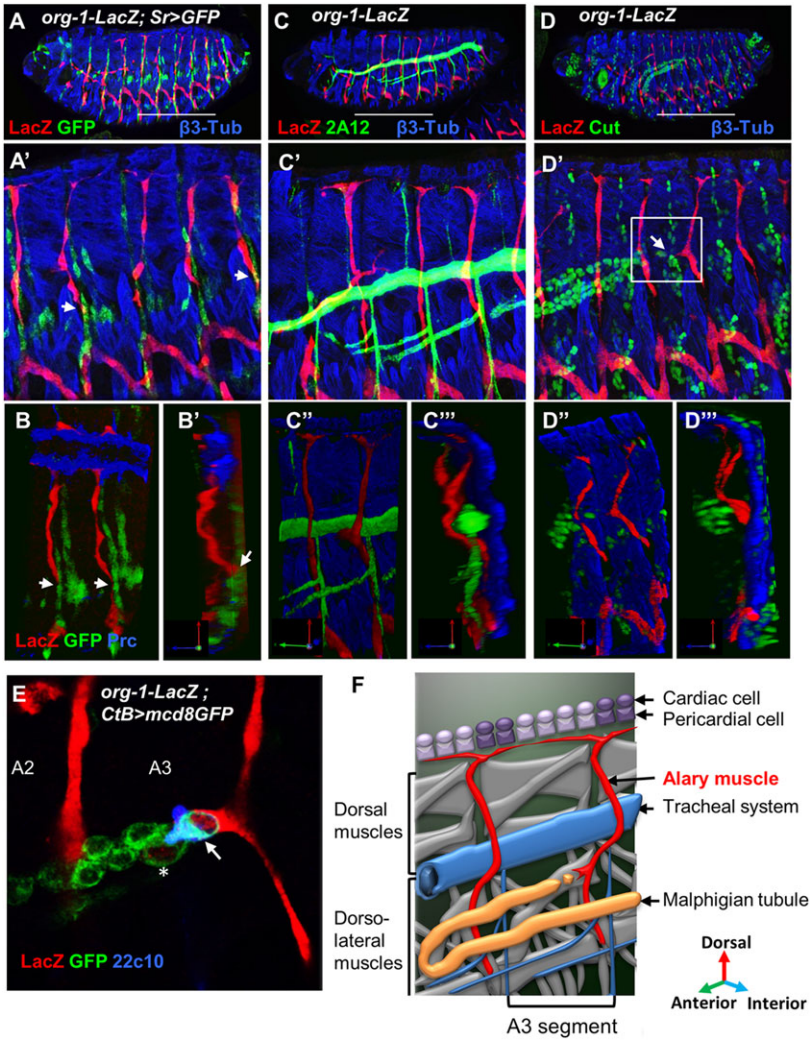

Fig. 2. Abdominal AMs connect multiple organs. (A-B′) Stage 16 *org-1-lacZ, sr-Gal4xUAS-mcd8GFP* (*sr>GFP*) embryos stained for β-gal (red) and GFP (green) to visualize the AM and the tendon cells, respectively, and either β3-Tub (A,A′) or Prc (B,B′) (blue) to visualize somatic muscles and the ECM surrounding pericardial cells, respectively. Epidermal attachment sites of AMs are indicated by arrows. (A) Whole embryo. (A′) Enlarged view of five adjacent abdominal segments (white bar in A). (B,B′) Three-dimensional reconstructions of two adjacent segments; (B) internal, (B′) transverse view. (C,D) Staining *org-1-lacZ* embryos for β-gal and 2A12 (C) or Cut (D) (green) to visualize tracheal branches and MT cells, respectively. (C′,D′) Magnified views. (C″,D″,C‴,D‴) Three-dimensional reconstructions of two segments showing internal and transverse views. (E) Detailed view of the interaction between the MT tip cell and the AM in A3 (boxed in D′); *org-1-lacZ; CtB-Gal4; UAS-mcd8GFP* embryo, stained for β-gal (red), GFP (green) and 22c10 (blue) to reveal the membrane of MT cells and the tip cell. Both the tip cell (arrow) and its sibling (asterisk) are *org-1-lacZ* positive. (F) Connections established by the AM in the third abdominal segment, dorsally to the cardiac tube, laterally to tendon cells, and internally to the MT tip cell (viewed from inside as in C″). AMs maintain the tracheal dorsal trunk close to the somatic muscles. The green, red and blue arrows indicate anteroposterior, dorsoventral and external-to-internal axes of the embryo, respectively.

that it is the tip cell sibling and, by inference, that *org-1-lacZ* (Org-1) is expressed in the tip cell progenitor. Weavers and Skaer (2013) showed that adhesion between the MT tip cell and AMs is required for the looped architecture and normal dorsal positioning of anterior MTs; when either the tip cell is not specified or AMs are laser ablated, the anterior MTs are misshapen and extend too far into the anterior of the embryo. Since AMs are missing or severely malformed in *org-1* mutant embryos (Schaub et al., 2012), a similar MT phenotype might have been expected. However, we observed a more severe phenotype – that is, a posterior shifting of the MT kink and tip cell position (supplementary material Fig. S3). This more severe phenotype suggests that, apart from being required for AM development, Org-1 could play a specific role at the MT tip. *org-1* is also required for Dpp expression in the visceral mesoderm, which serves as a cue for anterior migration of the kinked portion of the MTs (Schaub and Frasch, 2013; Weavers and Skaer, 2013). Hence, the observed MT phenotype is explicable by a cumulative defect of disrupted anterior guidance, absence of the attachment substratum of the tip cells, and the failure of the tip cells to attach to alternative targets.

In summary, our analysis of AM morphology in fully developed embryos shows that AMs attach to the dorsal vessel, run internally to the dorsal branch of tracheae and anchor ventrally to epidermal tendon cells. In addition, the AM in A3 anchors the tip cell of the anterior MT at the end of embryogenesis. Altogether, these topological connections suggest a role of AMs in maintaining the proper anatomical organization of different internal organs of the larva (Fig. 2F).

TARMs connect multiple organs

Unlike AMs, which are vertical and run along the abdominal segmental borders, TARMs display oblique orientations and straddle several adjacent segments. In order to describe their morphology in detail, we used the same markers as for AMs plus markers of the visceral muscles. Stage 16 embryos stained for *org-1-lacZ*, *sr>GFP* and β3-Tub showed that the TARMs connect to tendon cells along the posterior boundary of segments T1 and T2. We designate them as $TARM^{T1}$ and $TARM^{T2}$. At this stage, no TARM is observed in T3. Like AMs in abdominal segments, $TARM^{T2}$ attaches close to the SBM/DO3/DO4 attachment sites, and $TARM^{T1}$ close to the DO3/DO4/LA1/LA2 attachment sites, with no SBM being formed in T1 (Fig. 3A,A′). 2A12 staining showed that, similar to AMs, TARMs run internally to the dorsal branch of the trachea in the thoracic region. Closer examination showed that this branch, which supplies oxygen to the pharyngeal muscles, loops around $TARM^{T1}$, with a 90° rotation (Fig. 3B,B′,G). Three-dimensional reconstructions showed that the posterior attachment sites of $TARM^{T1}$ and $TARM^{T2}$ are located deep inside the embryo. Triple staining for *org-1-lacZ*, Fasciclin III (FasIII) and Mesh (Fig. 3C,F), and double staining for *HLH54F-RFP*, *org-1-RFP* and *MHC-tauGFP* (Fig. 3D,E), to visualize visceral muscles

Development (2014) 141, 3761-3771 doi:10.1242/dev.111005

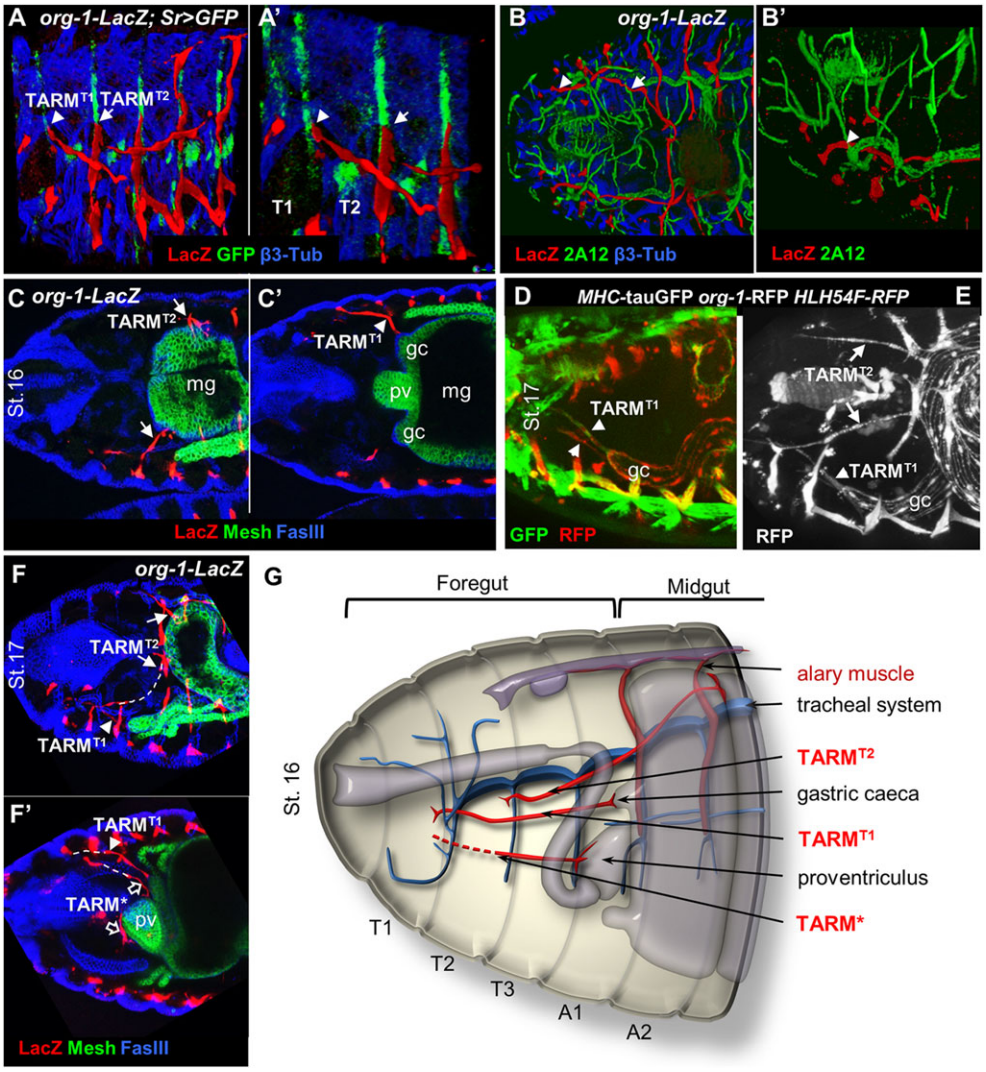

Fig. 3. Characterization of TARMS. (A) Three-dimensional reconstruction of lateral views of the T2-T3 and A1-A2 segments of stage 16 *org-1-lacZ, sr>GFP* embryos stained for β-gal (red), GFP (green) and β3-Tub (blue), visualizing TARM^{T1} (arrowhead) and TARM^{T2} (arrow), tendon cells and somatic muscles, respectively. (A′) Magnified view showing attachment of TARM^{T1} and TARM^{T2} to tendon cells along the posterior boundary of T1 and T2, respectively. (B) Three-dimensional reconstruction of a dorsal view of *org-1-lacZ* embryos stained for β-gal (red), β3-Tub (blue) and 2A12 (green) to visualize tracheae. (B′) Magnified view, showing how the dorsal tracheal trunk loops around TARM^{T1} (arrowhead). (C,C′) Dorsal views of a stage 16 *org-1-lacZ* embryo stained for β-gal (red), FasIII (blue) and Mesh (green) to visualize the midgut (mg), gastric caeca (gc) and proventriculus (pv). External (C) and internal (C′) views are shown of the same embryo with two distinct *z* foci. (D,E) Unfixed stage 17 embryos expressing (in addition to *org-1*-RFP) *MHC*-tauGFP in all muscles and *HLH54F*-RFP in longitudinal visceral muscle fibers that flank the midgut and gastric caeca. Dorsolateral views, with (D) internal sections only and (E) GFP channel omitted for clarity. (F,F′) Stage 17 embryo stained as in C. TARMs are represented by a dashed line when out of focus. (D,E,F) TARM^{T1} and TARM^{T2} connect the gastric caeca and the midgut at the first constriction level, respectively. (F′) A third pair of alary-related muscles, termed TARM* (open white arrow), connect the proventriculus. (G) Summary of TARM^{T1}, TARM^{T2} and TARM* connections to different regions of the midgut. The dorsal trachea loops around TARM^{T1}.

and the midgut epithelium as well as the outer epithelial layer of the proventriculus (Izumi et al., 2012), showed that TARM^{T2} connects to the gut at the position of the first constriction, before any morphological sign of its invagination (Fig. 3C). At this stage, TARMs^{T1} make head-on contacts with the primordia of the gastric caeca (Fig. 3C′,G). These connections are integrin positive (supplementary material Fig. S2C) and are maintained at stage 16/17, when gut constrictions have resolved into loops, via βPS-integrin-dependent attachments (Fig. 3D,E; and data not shown). Rotation of the gut in connection with loop formation (Okumura et al., 2010) results in stretching of the TARMs and bilateral asymmetry of their left and right anchoring sites (Fig. 3F,F′; supplementary material Fig. S2). Through these experiments, we noticed the existence of a third pair of myofibers expressing Tup and Org-1, which connect to the proventriculus (Fig. 3F′,G; supplementary material Fig. S4). As we have identified neither its anterior attachment site nor its PC, this myofiber, named TARM*, was not considered further in this work.

In conclusion, TARMs bridge different midgut regions to the exoskeleton, while intertwining with cephalic tracheal branches. Based on anatomy, we hypothesize that AMs and TARMs could contribute to maintaining organs in their proper positions during larval foraging movements.

AM and TARM lineage analyses

Org-1 is expressed in the AM progenitor at late embryonic stage 11 (Schaub et al., 2012). Staining embryos at that stage for Tup and *rp298(duf)-lacZ*, a marker of muscle PCs and FCs (Nose et al., 1998),

Development (2014) 141, 3761-3771 doi:10.1242/dev.111005

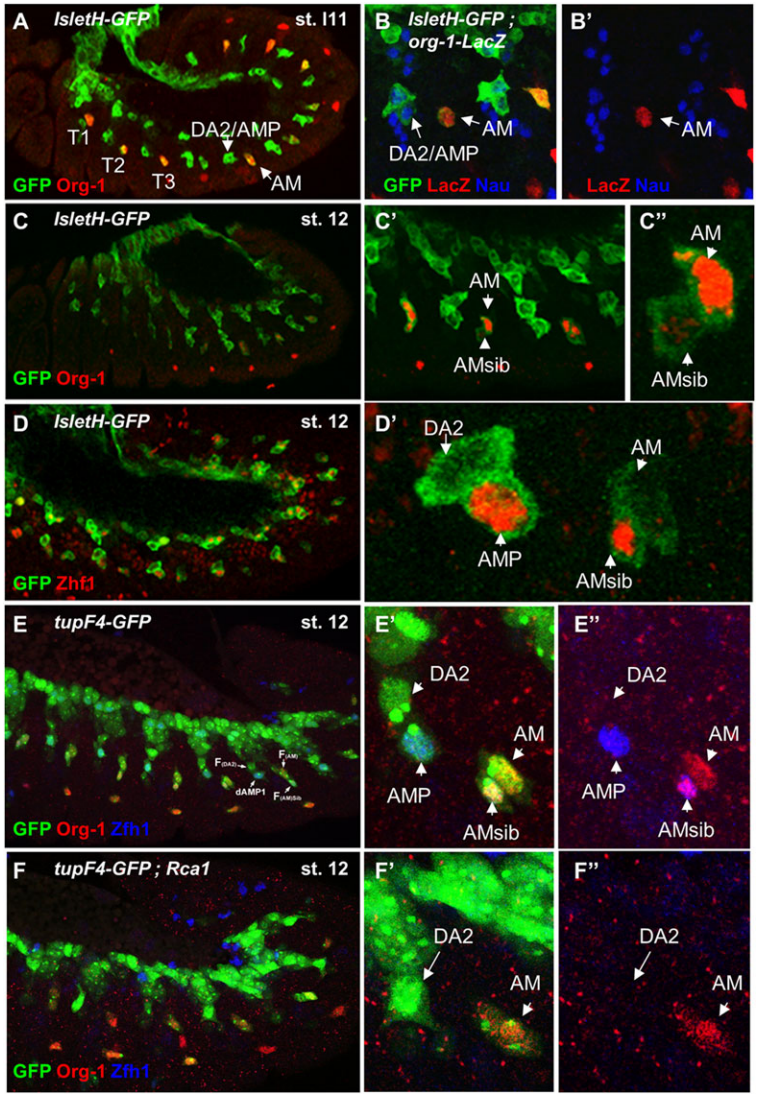

Fig. 4. The AM lineage. (A) Late stage 11 *IsletH-GFP* embryo stained for GFP (green) and Org-1 (red), showing one double-positive cell in each T1-T3 and A1-A7 segment. (B,B′) *IsletH-GFP; org-1-lacZ* embryo stained for GFP (green), β-gal (red) and Nau (blue); one A segment is shown. Positions of the DA2/AMP and AM PCs are indicated. (B′) Red and blue channels. (C,D) Stage 12 *IsletH-GFP* embryos stained for GFP and either Org-1 (C) or Zfh1 (D) (red). (C′,C″,D′) Magnifications of C and D. The AM FC remains Org-1 positive, whereas its sibling expresses Zfh1. (E,F) Stage 12 *tupF4-GFP* (E) and *tupF4-GFP, Rca1* (F) embryos stained for GFP, Org-1 (red) and Zfh1 (blue). (E′,E″,F′,F″) Magnifications of E and F, with E″ and F″ showing only the red and blue channels. Zfh1 expression is lost in *Rca1* embryos.

identified the four PCs at the origin of the DA1, DO2, DO1 and DA2 dorsal muscles, plus another cell located several cell diameters posterior to the DA2/AMP PC (Boukhatmi et al., 2012). Double staining for Org-1 and *IsletH-GFP* shows that this cell is the AM progenitor and is segmentally repeated along the posterior/anterior segmental border (Fig. 4A; supplementary material Fig. S5). Double staining for *org-1-lacZ* and Nau showed that the AM PCs do not express Nau, in contrast to the dorsal body wall muscle PCs/FCs (Fig. 4B,B′).

The AM PC divides at stage 12, with one daughter cell remaining Org-1 positive (Fig. 4C-C″). Double staining for *IsletH-GFP* and Zfh1, a general AMP marker (Sellin et al., 2009; Figeac et al., 2010), previously established that the DA2 PC gives rise to a mixed DA2/AMP lineage (Boukhatmi et al., 2012). Similarly, one AM PC daughter cell is Zfh1 positive (Fig. 4D,D′). Triple staining for Org-1, Zfh1 and *tupF4-GFP* confirmed that asymmetric division of the AM PC gives rise to one daughter that remains Org-1 positive and a sibling that is Zfh1 positive (Fig. 4E-E″). Muscle PC into FC divisions do not occur in *Regulator of cyclin A1* (*Rca1*) mutant embryos, and *Rca1* mutations were obtained in an EMS screen utilizing *org-1-RFP* as a marker for abnormal development of AMs [and LO1/VT1/SBM muscles (Hollfelder et al., 2014)]. Triple staining of *Rca1* embryos showed that, in the absence of division, the AM PC remains Org-1 positive and Zfh1 negative (Fig. 4F-F″), indicating that the AM fate is its default fate. Zfh1 staining does not persist in the AM sibling, unlike in the DA2 sibling (data not shown), and the ultimate fate of this cell remains unclear.

To follow the differentiation of the AM FC into muscle fiber, we performed time-lapse imaging of live embryos, as well as Org-1/*tup-GFP* staining (supplementary material Fig. S5). For this analysis, we used an AM-specific enhancer, *tupAME-GFP* (see below). Both approaches showed that AM FCs extend filopodial extensions along the dorsoventral axis and start fusing with myoblasts to form syncytial fibers that elongate until they connect dorsally to the heart and ventrally to the lateral epidermis (supplementary material Fig. S5 and Movie 1). In the abdominal segments A1-A7, each AM PC/FC gives rise to a mature AM. However, although one Org-1^{+}/Tup^{+}cell is specified in each thoracic segment (Fig. 4A), only two TARMs, namely TARM^{T1} and TARM^{T2}, develop in the thorax (Fig. 1B, Fig. 3G), raising the question of the fate of the T3 progenitor. To address this question, we used *org-1-lacZ* in combination with the reporter line *tupADME-lacZ*, which allows TARMS to be distinguished (β-gal^{+}, GFP^{+}) from other tissues expressing only one reporter. These experiments showed that TARM^{T1} and TARM^{T2} grow and extend posteriorly between stage 13 and 14, whereas TARM^{T3} stays globular and

Development (2014) 141, 3761-3771 doi:10.1242/dev.111005

disappears, probably by apoptosis, at stage 14 (supplementary material Fig. S6).

In conclusion, lineage analyses and imaging of co-expressed Org-1/Tup during muscle development shows that AMs and TARMs constitute homologous muscle lineages in abdominal A1-A7 and T1-T2 segments, respectively, and that this lineage is abortive in T3.

org-1 acts upstream of *tup* in AM development

Double staining of *tup*^{ex4}*; org-1-lacZ* embryos (de Navascues and Modolell, 2010) for β3-Tub and β-gal showed that AMs form in the absence of Tup activity but are severely malformed, whereas TARMs are essentially missing (Fig. 5A-B′). The patterns of expression and mutant phenotypes of *tup* and *org-1* raised the question of whether *tup* was acting in parallel or downstream of *org-1*. We first stained stage 11-12 *tup*^{ex4} embryos for Org-1 and observed that Org-1 expression in AM and TARM progenitors was unaffected (not shown). We then analyzed Tup expression in AM progenitors in *org-1*^{OJ487} embryos using, as an internal reference, DA2/AMP expression. Specific loss of Tup expression in a significant fraction of AM progenitors indicated that Org1 regulates *tup* expression (Fig. 5C,D).

Two separate *tup* CRMs, namely *IsletH/tupF4* and *tupDME* (dorsal muscle enhancer), drive expression in both dorsal muscles and AMs (see Fig. 6A). *tupF4* activity is detected at late stage 11 in the DA2 and AM PCs, whereas *tupDME* starts to be detectable at stage 12 and remains active in the AMs and dorsal muscles up to stage 16 (Boukhatmi et al., 2012) (Fig. 5E,G). We observed complete loss of *tupDME-lacZ* expression in AM PCs and FCs in *org-1* mutant embryos (Fig. 5F). Staining stage 16 embryos confirmed that, in the absence of *org-1*, both Tup (not shown) and *tupDME-lacZ* expression is completely lost in AMs, while remaining normal in body wall muscles (Fig. 5G,H).

To further assess whether Org-1 regulation of *tup* is AM specific, we expressed Org-1 in the entire mesoderm [*2xPE>org-1* (Schaub et al., 2012)] and examined Tup expression using both antibodies and the AM reporter line, *tupADME*$^{\Delta Tup}$ (see below and Fig. 6A). We observed a thickening of AMs and TARMs, with more Tup-positive nuclei per fiber than in wild type and, in some of segments, the formation of one extra muscle with an AM-like morphology (Fig. 5I,J). Although the thickening phenotype might reflect a differentiation phenotype, duplications of AMs suggested that pan-mesodermal expression of Org-1 is able to convert the AM FC sibling to an AM fate and that the ability of Org-1 to activate Tup is restricted

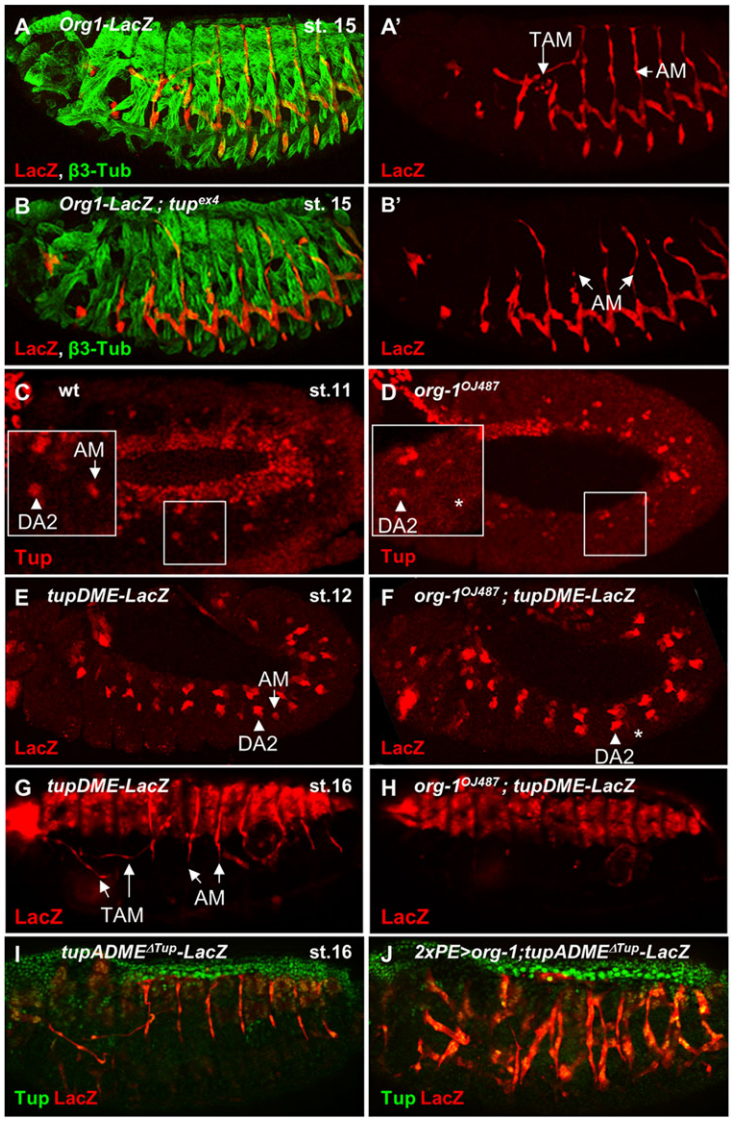

Fig. 5. *tup* AM and TARM mutant phenotypes and *org-1>tup* epistasis. (A-B′) Stage 15 *org-1-lacZ* (A) and *org-1-lacZ; tup*^{ex4} (B) embryos stained for β3-Tub (green) and β-gal (red). The AMs are distorted and TARMs are missing in *tup*^{ex4} embryos. (C,D) Stage 11 wild-type (C) and *org-1*^{OJ487} (D) embryos. Tup expression (red) is specifically lost in the AM lineage. (E-H) *tupDME-lacZ* expression in wild-type (E,G) and in *org-1*^{OJ487} (F,H) embryos at stage 12 (E,F) and 16 (G,H). Reporter expression is lost in the AM lineage from the PC stage in *org-1*^{OJ487} embryos (asterisk). (I,J) Stage 16 *tupADME*$^{\Delta Tup}$*-lacZ* (I) and *tupADME*$^{\Delta Tup}$*-lacZ; 2xPE>>org-1* (J) embryos stained for Tup (green) and β-gal (red). AM duplications are observed upon pan-mesodermal expression of Org-1.

Development (2014) 141, 3761-3771 doi:10.1242/dev.111005

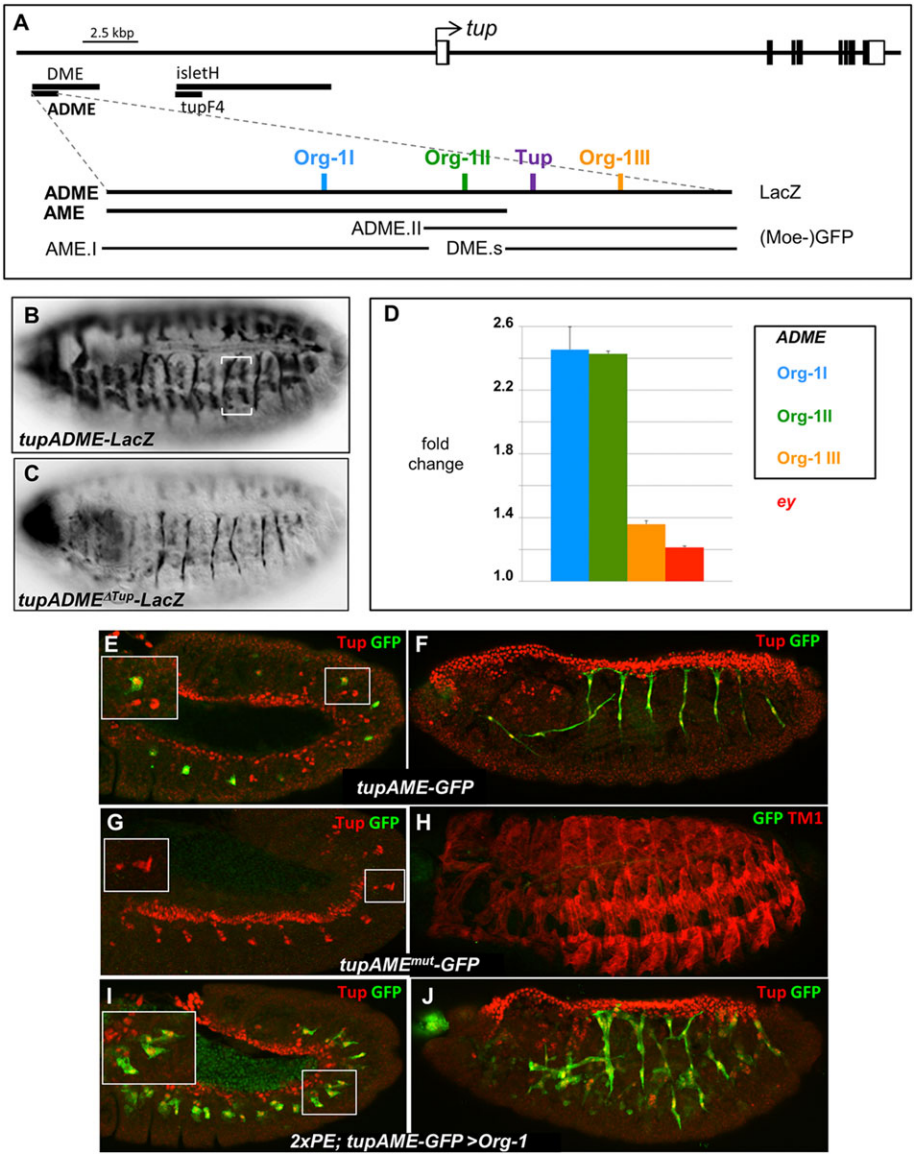

Fig. 6. Org-1 directly regulates a *tup* AM/TARM-specific CRM. (A) (Top) The genomic position of *tup*, with the transcription start indicated by an arrow and coding exons by boxes; the positions of the *IsletH*, *tupF4*, *tupDME* and *tupADME* CRMs are indicated. (Bottom) Positions of truncated versions of *tupADME* fused to *moeGFP*. Predicted binding sites for Tup and Org-1 are indicated and numbered. (B,C) β-gal staining shows the specific decrease of *tupADME-lacZ* expression in dorsal muscles (bracketed in B) when the Tup binding site is mutated (C). (D) Anti-Org-1 ChIP with chromatin from *2xPE; 24B>>org-1* embryos was assayed by qPCR using amplicons covering each of the predicted binding sites I to III present in *tupADME*. Each bar represents the average of three independent biological replicates normalized to negative controls from the C15 gene. An eyeless (*ey*) exonic amplicon serves as an additional negative control. Error bars indicate s.d. (E,F) *tupAME-moeGFP* stage 11 (E) and 16 (F) embryos stained for GFP (green) and Tup (red). *tupAME* activity recapitulates Tup expression in AMs and TARMs. (G,H) *tupAME* activity is lost when both Org-1 binding sites (I and II) are mutated (*tupAME^{mut}-moeGFP*). Embryo in H is counterstained for Tropomyosin (TM1). (I,J) *tupAME-moeGFP* expression is specifically induced and duplicated AMs form upon pan-mesodermal Org-1 expression (*2xPE>org-1*).

to the AM and TARM lineages. To then determine the contribution of Tup activation to the *org-1* gain-of-function phenotype, we expressed Tup in the entire mesoderm (*2xPE>UAS-tup*). In contrast to Org-1, Tup overexpression does not provoke AM duplications (not shown), reinforcing the conclusion that Tup cannot substitute for Org-1 function in engaging the AM differentiation program.

In conclusion, mutant analyses show that both *org-1* and *tup* functions are required for AM and TARM development, with *org-1* acting upstream of *tup* specifically in these muscles and being instructive for the AM fate.

Org-1 is a direct upstream regulator of *tup* in AMs and TARMs

The Org-1-dependent activity of *tupDME* in AMs prompted us to study this enhancer in more detail. Based on the position of a meso-ChIP CRM (Sandmann et al., 2007; Zinzen et al., 2009) and sequence conservation between different *Drosophila* species, we first trimmed *tupDME* to a 1.3 kb DNA fragment, which we call *tupADME* (alary and dorsal muscle enhancer) (Fig. 6A). Bioinformatics indicated the presence of three potential Org-1 binding sites (Muller and Herrmann, 1997; Schaub et al., 2012), which we designated Org-1 I, II and III, as well as one Tup binding site (Fig. 6; supplementary material Fig. S7). Mutation of the predicted Tup binding site (*tupADME$^{\Delta Tup}$*) resulted in a decrease in enhancer activity in dorsal muscles but not in AMs (Fig. 6B,C). Therefore, Tup is required for maintaining its own expression via direct positive autoregulation in dorsal body wall muscles but not in AMs.

ChIP analysis with chromatin prepared from stage 11-12 embryos (Schaub et al., 2012) indicated *in vivo* Org-1 binding to Org-1 sites I and II (Fig. 6D). This suggested that Org-1 I and II could mediate direct *tup* regulation by Org-1. To test this hypothesis, we made reporter constructs in which shorter versions of *tupADME* were fused to *moeGFP* (Fig. 6A). A subfragment containing Org-1 I and II, called *tupAME* (alary muscle enhancer), is active in AMs and TARMs but not in dorsal muscles (Fig. 6E,F, Fig. 7). Mutation of both Org-1 I and II completely abolished *tupAME* activity (*tupAME^{mut}*; Fig. 6G,H), demonstrating that Org-1 regulation of *tup* expression in AMs/TARMs is direct. Pan-mesodermal expression of Org-1 led to Tup and *tupAME* expression in two adjacent cells per segment (mean=1.91±0.44, *n*=90), instead of one in wild-type embryos (0.93±0.25, *n*=45), at stage 12, correlating with AM duplications and supporting our proposal of a conversion

Development (2014) 141, 3761-3771 doi:10.1242/dev.111005

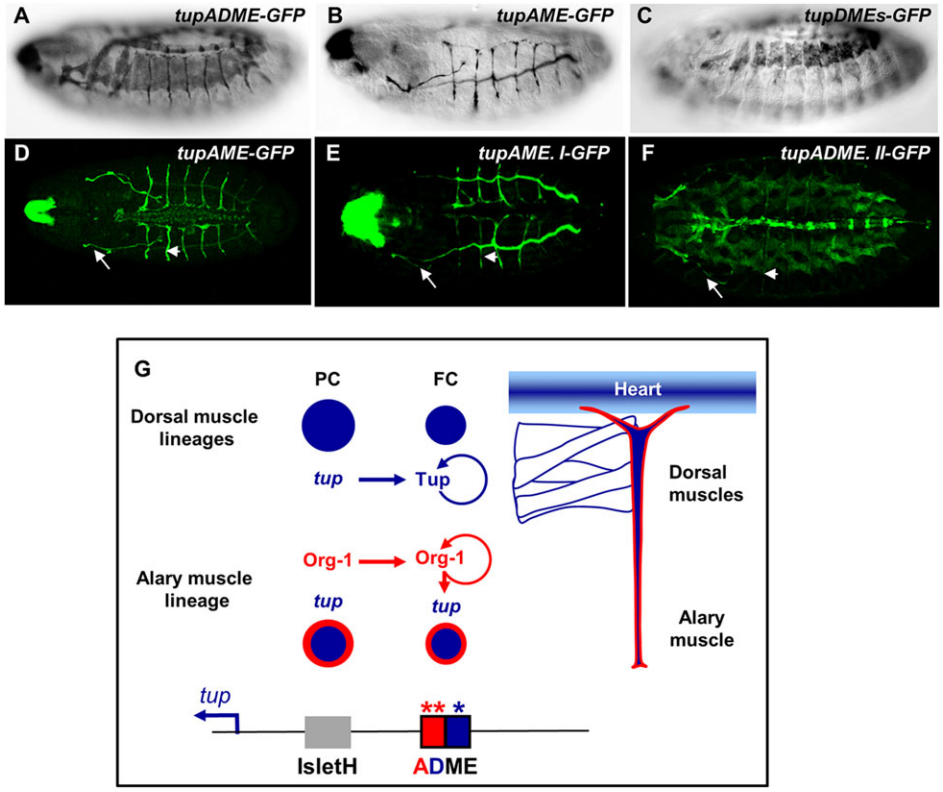

Fig. 7. Lineage-specific direct regulation of *tup* by distinct Org-1-dependent and Tup-dependent CRMs. (A-C) Stage 15 *tupADME-moeGFP* (A), *tupAME-moeGFP* (B) and *tupDMEs-moeGFP* (C) embryos stained for GFP, showing the separation of the AM (B) and dorsal muscle (C) CRMs. (D-F) Dorsal view of stage 16 *tupAME-moeGFP* (D), *tupAME.I-moeGFP* (E) and *tupADME.II-moeGFP* (F) embryos. Each of the Org-1 I and II binding sites is active in AMs and TARMs (arrows). (G) The lineage diversity of transcriptional regulatory networks patterning the larval dorsal musculature. Tup expression (blue) is driven by the *tupF4*/*IsletH* CRM in the heart, dorsal somatic muscle and AM progenitors. Maintenance of *tup* expression depends on direct autoregulation in dorsal muscles and on direct regulation by Org-1 (red) in AM/TARMs, via two separate, DM-specific and AM-specific CRMs. Asterisks indicate the positions of the Org-1 and Tup binding sites.

of the AM FC sibling to an AM fate (Fig. 6I,J; Fig. 5J). This confirmed that the ability of Org-1 to activate *tup* expression is specific to the AM PC or/and daughter cells. A shorter version of *tupADME* termed *tupDME.s*, which removes Org-1 I and II but preserves Org-1 III (Fig. 6A), loses expression in AMs (Fig. 7C), confirming that the Org-1 III site, which is not actively bound by Org-1 *in vivo*, is not functional.

The presence of two sites bound by Org-1 *in vivo* raised the question of whether these are redundant or, alternatively, could be specific for either AMs or TARMs. To address this question, we constructed two additional reporters termed *tupAME.I* and *tupADME.II* fused to *moeGFP* (Fig. 6A). *tupAME.I* is only active in AMs and TARMs (and in ectodermal cells connecting the frontal sac and pharynx, as with its parental construct), whereas *tupADME.II* is also active in the heart and dorsal muscles, consistent with the presence of the Tup autoregulatory site in this fragment. Both constructs are able to drive GFP expression in both AMs and TARMs, although much more weakly than *tupAME*, showing that both Org-1 I and II are functional and are both required for robust expression (Fig. 7D-F).

Together, these results allow us to draw a schematic model of *tup* regulation in AMs in comparison to dorsal body wall muscles, which highlights the key role of lineage-specific autoregulation during patterning of the *Drosophila* larval dorsal musculature (Fig. 7G).

DISCUSSION

The anatomical organization of the *Drosophila* larval organs is established during embryogenesis. We show here that abdominal AMs and their thoracic counterpart, the TARMs, establish physical connections between the exoskeleton and different internal organs, and that TARMs thus represent a novel type of muscle. The control of AM and TARM development by Org-1 and Tup – as orthologs of Tbx1 and Islet1, two key transcription factors of cardiopharyngeal mesoderm development in vertebrates – suggests that these transcription factors were part of an ancestral regulatory kernel that was redeployed several times during evolution to control different embryonic mesoderm derivatives.

AMs and TARMs: homologous muscle lineages with morphologies that depend upon Hox input

Seven pairs of embryonic abdominal AMs connect to the heart and the aorta. Interestingly, pan-mesodermal expression of either Ubx or AbdA, two abdominal Hox proteins, resulted in the formation of three supernumerary pairs of AMs arranged in a segmental pattern in the three thoracic segments (LaBeau et al., 2009). This suggested the existence of thoracic PCs that fail to give rise to muscles in the absence of proper Hox input. Such a scenario accounted for the lack of DA3 muscle in the T1 segment (Enriquez et al., 2010). Alternatively, these thoracic PCs could give rise to previously unrecorded muscles. We discovered that both explanations apply. Thoracic Org-1^{+}/Tup^{+} PCs give rise to a novel type of muscles, which we call TARMs. Only TARM^{T1} and TARM^{T2} form during normal development, whereas TARM^{T3} differentiation is abortive. We also noted that an extra pair of muscles expressing both *org* and *tup* reporter genes in late embryos attaches to the proventriculus. The PCs at the origin of this extra pair of muscles, which we named TARM*, remain to be identified.

In summary, TARMs and AMs are generated by homologous lineages and form thin, elongated muscles of characteristic morphology and attachment sites that integrate segment-specific information.

AMs and TARMs and the anatomical organization of the larva

Descriptions of AMs in adults of different insects led to proposals of their role in either maintaining the position of the heart, regulating

Development (2014) 141, 3761-3771 doi:10.1242/dev.111005

the hemolymph flow and/or controlling heart beat. The requirement of transient contacts between some AMs and the distal tip cell of MTs revealed yet another role of AMs, namely for proper bending and positioning of MTs (Weavers and Skaer, 2013). We show here that, through linking the lateral epidermis to the dorsal vessel, AMs press the dorsal, main branch of the trachea towards the body wall. TARMs also establish intimate topological relations with cephalic branches of the trachea in their trajectory from thoracic lateral epidermis/exoskeleton to specific regions of the midgut. Rotation of the gut at the end of embryogenesis (Okumura et al., 2010) results in stretching and bilateral asymmetry of the left and right TARMs. This suggests that TARMs have elastic properties, as already indicated by their transient deformation upon interaction with the MT tip cell (Weavers and Skaer, 2013).

Although the function of AMs and TARMs during larval development and growth remains to be fully assessed, the morphological and elastic properties of AMs and TARMs suggest that they could be involved in controlling the position of the heart, trachea and gut during larval foraging movements. Whereas Org-1 and Tup are only co-expressed in the AM/TARM lineage, each is expressed in several other mesodermal or non-mesodermal tissues, precluding the use of mutants to selectively study AM and TARM function. Whether AMs and TARMs represent a new type of muscle with both spring-like and contractile properties is one of the questions to be addressed henceforth.

Direct regulation of *tup* by Org-1 is AM/TARM-specific

The morphological properties specific to each *Drosophila* body wall muscle are determined by the expression of specific combinations of iTFs in each FC and derived muscle (de Joussineau et al., 2012). Lineage specificity involves positive and negative cross-regulations between different iTFs, as well as iTF autoregulation. The maintenance of Org-1 and Tup expression in body wall muscles depends upon autoregulation (Boukhatmi et al., 2012; Schaub et al., 2012). We show here that *tup* autoregulation in dorsal muscles is direct, but does not operate in AMs; here, *tup* is directly regulated by Org-1. Org-1 directly regulates the expression of two other iTFs, namely *slouch* and *ladybird*, in other muscle lineages (Schaub et al., 2012). The AM/TARM Org-1>Tup hierarchy further underlines the intricate, combinatorial nature of transcriptional regulatory networks specifying *Drosophila* muscle identity. We have now identified an Org-1-dependent *tup* enhancer called *tupAME*, which is only active in AMs/TARMs and ectodermal cells connecting the frontal sac and pharynx. This CRM should provide a means to specifically target expression and modify AMs/TARMs in order to assess their function in larvae.

New parallels between the transcriptional regulatory networks patterning *Drosophila* and vertebrate muscles?

Nkx2.5, Tbx1 and Islet1 are major actors in the vertebrate genetic program controlling early heart and pharyngeal muscle development from common progenitors lying in the second heart field (SHF) in chordates (Cai et al., 2003; Prall et al., 2007; Sambasivan et al., 2009; Kelly, 2012; Watanabe et al., 2012). NK4/Nkx2.5 was recently shown to antagonize Tbx1 and repress EBF/COE function to promote cardiac versus pharyngeal muscle fate in the ascidian SHF, with Islet1 being expressed in both derivatives (Wang et al., 2013; Razy-Krajka et al., 2014). In the *Drosophila* embryo, the orthologs of Nkx2.5 and Islet1 are required for the formation of all (in the case of Tin) or some (in the case of Tup) of the dorsal mesodermal derivatives (heart, dorsal body wall muscles, visceral muscles, lymph gland) (Azpiazu and Frasch, 1993; Bodmer, 1993; Zaffran et al., 2006; Mann et al., 2009). Moreover, Tup represses the COE ortholog Collier (Col; Knot – FlyBase) in dorsal muscles (Boukhatmi et al., 2012), and Org-1/Tbx1 is expressed in some body wall muscles, the AMs and the visceral mesoderm, although not in myocardial progenitors. Together, these findings suggest that the Nkx2.5/Tin, Tbx1/Org-1, Islet1/Tup and COE/Col transcription factors are part of an ancestral regulatory kernel controlling diversification of heart and muscle lineages from a common progenitor pool. Future studies will be required to establish which ancestral interactions have been redirected to foster the emergence of insect AMs and TARMs.

To our knowledge, no striated muscle has been described so far to connect the (exo)skeleton to the gut, either in insects or in vertebrates. In mammals, lung and heart are separated from visceral organs by the diaphragm muscle. However, a muscular diaphragm is a defining characteristic of mammals that is not found in other vertebrates, and the ancestral origin of this recent innovation is currently unknown (Merrell and Kardon, 2013). Although highly speculative, it will be interesting to investigate whether the vertebrate muscle/septum and the insect AMs/TARMs could represent two specific adaptations of an ancestral demarcation between the circulatory systems, respiratory systems and visceral organs.

MATERIALS AND METHODS

Drosophila strains

All *Drosophila melanogaster* stocks were grown on standard medium at 25°C. Strains used: tup^{ex4} (de Navascues and Modolell, 2010), $org\text{-}1^{OJ487}$, *org-1-HN39-lacZ*, *UAS-org-1*, *2xPE-Gal4; how*^{24B}*-Gal4* (Schaub et al., 2012), *IsletH-GFP* (Thor and Thomas, 1997), *tupF4-GFP* (Tao et al., 2007), *tupDME-lacZ* (Boukhatmi et al., 2012), *sr-Gal4* (obtained from T. Volk, Weizmann Institute of Science, Rehovot, Israel), *CtB-Gal4* (Sudarsan et al., 2002), $Rca1^{S0844}/Rca1^{S2926}$ (I.R., unpublished; used in the heterozygous condition), *HLH54Fb-RFP* (Ismat et al., 2010), *MHC-tauGFP* (Chen and Olson, 2001), *UAS-mcd8GFP* and *UAS-tup* (Bloomington Stock Center). Mutants were balanced over marked chromosomes: *FM7 ftz-lacZ*; *CyO wg-lacZ*; *TM3 twi-lacZ* and homozygotes identified by the absence of β-gal expression. Pan-mesodermal expression of *UAS-org-1* with *2xPE-GAL4;how*^{24B}*-GAL4* was carried out at 28°C.

Construction of transgenic reporter lines

For *tup* reporter lines, the genomic regions chr2L: 18897397..18900688 (*tupADME*) and chr2L: 18899851..18900688 (*tupAME*) according to FlyBase release R5.42 were amplified using *yw* genomic DNA as template. *tupADME* was cloned into the *attB-inslacZ* vector (Enriquez et al., 2010). *tupAME* was recombined into *pDEST-MoeGFP*. Positions of *tupADME* subfragments used for additional reporter lines are indicated in supplementary material Fig. S7. For creation of $tupAME^{mut}$*-moeGFP*, Org-1 binding sites were predicted using Target Explorer (Sosinsky et al., 2003) with a positional weight matrix generated by SELEX (Schaub et al., 2012), and mutated by site-directed mutagenesis as follows: *tupAME* TAACACAT → *tupAME-orgImut* TAAGCTTT; and *tupAME* GGGTGCCA → *tupAME-orgIImut* GGCTCGAG. Mutagenesis of the consensus Tup recognition sequence CTAATG (Portales-Casamar et al., 2010) to CTAGGT was achieved by PCR. The *lacZ* and *moeGFP* reporters were inserted at position 68A4 on the third chromosome by injection into *nos-phiC31-NLS; attP2* embryos (Bischof et al., 2007; Markstein et al., 2008).

Immunohistochemistry and time-lapse imaging of GFP/RFP reporters

Immunostaining of whole-mount embryos was performed using standard techniques. The following primary antibodies were used: chicken anti-β-gal (1:2000; Abcam, ab9361); mouse anti-GFP (1:100; Roche, 11814460001); anti-β-gal (1:1000; Promega, Z3783, Lot 25580607); anti-TM1 (1:200; Babraham Institute, Cambridge, UK, MAC 141); mouse anti-Tup (1:100), anti-Prc (1:500), anti-Cut (1:200), anti-FasIII (1:20), anti-βPS (1:10), 22c10

(Futsch – FlyBase) (1:50) and 2A12 (Pavarotti – FlyBase) (1:5), all from Developmental Studies Hybridoma Bank; rabbit anti-GFP (1:500; Torrey Pines Biolabs, TP401, Lot 071519); anti-Nau (1:100; Bruce Paterson, Bethesda, USA); anti-Zfh1 (1:5000; Ruth Lehmann, New York, USA); anti-β3-Tub (1:5000; Renate Renkawitz-Pohl, Marburg, Germany); anti-Mesh (1:1000) (Izumi et al., 2012); and rat anti-Org-1 (1:100) (Schaub et al., 2012). Secondary antibodies were Alexa Fluor 488, 647 or 555 conjugated (1:300; Molecular Probes). Optimized confocal sections were acquired on a Leica SP5 or SPE microscope. Projections and three-dimensional reconstructions were created using ImageJ (NIH) and Volocity (PerkinElmer) software, respectively. Time-lapse imaging of embryos carrying *GFP* and *RFP* reporter genes was performed as previously described (Hollfelder et al., 2014).

Chromatin immunoprecipitation (ChIP) assays

ChIP experiments were performed using stage 11-15 *2xPE; how^{24B}>>UAS-org-1* embryo collections and Org-1 antibodies as described (Schaub et al., 2012). The precipitated DNA was quantified in triplicate using FastStart Universal SYBR Green Master (Rox) (Roche Applied Science) on an Eco Real-Time PCR System (Illumina). Three independent precipitations per amplicon were analyzed.

Acknowledgements

We thank the Bloomington Stock Center and colleagues for *Drosophila* strains; Mikio Furuse, Alain Garces, Bruce Paterson and Renate Renkawitz-Pohl for antibodies; Michèle Crozatier and Alice Davy for helpful discussion and critical reading of the manuscript; Brice Ronsin at the Toulouse RIO Imaging platform; and Julien Favier for maintenance of fly stocks.

Competing interests

The authors declare no competing financial interests.

Author contributions

H.B., C.S., L.B., M.F. and A.V. conceived and designed the experiments. H.B., C.S., L.B., I.R. and J.L.F. performed the experiments. H.B., C.S., L.B., I.R., J.L.F., M.F. and A.V. analyzed the data. J.L.F. created images of AMs and TARMs. L.B. and A.V. wrote the manuscript.

Funding

This work was supported by Centre National de la Recherche Scientifique (CNRS), Ministère de l'Enseignement Supérieur et de la Recherche (MESR), Université Paul Sabatier, Association Française contre les Myopathies (AFM) and an Agence Nationale de la Recherche (ANR) grant [13-BSVE2-0010-0] to A.V.; and by Deutsche Forschungsgemeinschaft (DFG) grants to M.F. [FR696/3-1] and I.R. [RE 2985/1-1]. H.B. was supported by fellowships from MESR and Fondation pour la Recherche Médicale (FRM) and L.B. by a fellowship from AFM.

Supplementary material

Supplementary material available online at
http://dev.biologists.org/lookup/suppl/doi:10.1242/dev.111005/-/DC1

References

Ashe, H. L., Mannervik, M. and Levine, M. (2000). Dpp signaling thresholds in the dorsal ectoderm of the Drosophila embryo. *Development* **127**, 3305-3312.

Azpiazu, N. and Frasch, M. (1993). tinman and bagpipe: two homeo box genes that determine cell fates in the dorsal mesoderm of Drosophila. *Genes Dev.* **7**, 1325-1340.

Bate, M. (1993). The mesoderm and its derivatives. In *The Development of Drosophila melanogaster*, Vol. 2 (ed. M. Bate and A. Martinez-Arias) pp. 1013-1090. Cold Spring Harbor, NY: Cold Spring Harbor Laboratory Press.

Baylies, M. K., Bate, M. and Ruiz Gomez, M. (1998). Myogenesis: a view from Drosophila. *Cell* **93**, 921-927.

Bischof, J., Maeda, R. K., Hediger, M., Karch, F. and Basler, K. (2007). An optimized transgenesis system for Drosophila using germ-line-specific phiC31 integrases. *Proc. Natl. Acad. Sci. USA* **104**, 3312-3317.

Bodmer, R. (1993). The gene tinman is required for specification of the heart and visceral muscles in Drosophila. *Development* **118**, 719-729.

Boukhatmi, H., Frendo, J. L., Enriquez, J., Crozatier, M., Dubois, L. and Vincent, A. (2012). Tup/Islet1 integrates time and position to specify muscle identity in Drosophila. *Development* **139**, 3572-3582.

Cai, C.-L., Liang, X., Shi, Y., Chu, P.-H., Pfaff, S. L., Chen, J. and Evans, S. (2003). Isl1 identifies a cardiac progenitor population that proliferates prior to differentiation and contributes a majority of cells to the heart. *Dev. Cell* **5**, 877-889.

Chen, E. H. and Olson, E. N. (2001). Antisocial, an intracellular adaptor protein, is required for myoblast fusion in Drosophila. *Dev. Cell* **1**, 705-715.

Crozatier, M., Ubeda, J.-M., Vincent, A. and Meister, M. (2004). Cellular immune response to parasitization in Drosophila requires the EBF orthologue collier. *PLoS Biol.* **2**, e196.

de Joussineau, C., Bataillé, L., Jagla, T. and Jagla, K. (2012). Diversification of muscle types in Drosophila: upstream and downstream of identity genes. *Curr. Top. Dev. Biol.* **98**, 277-301.

de Navascués, J. and Modolell, J. (2010). The pronotum LIM-HD gene tailup is both a positive and a negative regulator of the proneural genes achaete and scute of Drosophila. *Mech. Dev.* **127**, 393-406.

Dulcis, D. and Levine, R. B. (2003). Innervation of the heart of the adult fruit fly, Drosophila melanogaster. *J. Comp. Neurol.* **465**, 560-578.

Enriquez, J., Boukhatmi, H., Dubois, L., Philippakis, A. A., Bulyk, M. L., Michelson, A. M., Crozatier, M. and Vincent, A. (2010). Multi-step control of muscle diversity by Hox proteins in the Drosophila embryo. *Development* **137**, 457-466.

Enriquez, J., de Taffin, M., Crozatier, M., Vincent, A. and Dubois, L. (2012). Combinatorial coding of Drosophila muscle shape by Collier and Nautilus. *Dev. Biol.* **363**, 27-39.

Figeac, N., Jagla, T., Aradhya, R., Da Ponte, J. P. and Jagla, K. (2010). Drosophila adult muscle precursors form a network of interconnected cells and are specified by the Rhomboid-triggered EGF pathway. *Development* **137**, 1965-1973.

Frasch, M. (1999). Controls in patterning and diversification of somatic muscles during Drosophila embryogenesis. *Curr. Opin. Genet. Dev.* **9**, 522-529.

Frommer, G., Vorbruggen, G., Pasca, G., Jackle, H. and Volk, T. (1996). Epidermal egr-like zinc finger protein of Drosophila participates in myotube guidance. *EMBO J.* **15**, 1642-1649.

Glenn, J. D., King, J. G. and Hillyer, J. F. (2010). Structural mechanics of the mosquito heart and its function in bidirectional hemolymph transport. *J. Exp. Biol.* **213**, 541-550.

Hollfelder, D., Frasch, M. and Reim, I. (2014). Distinct functions of the laminin beta LN domain and collagen IV during cardiac extracellular matrix formation and stabilization of alary muscle attachments revealed by EMS mutagenesis in Drosophila. *BMC Dev. Biol.* **14**, 26.

Ismat, A., Schaub, C., Reim, I., Kirchner, K., Schultheis, D. and Frasch, M. (2010). HLH54F is required for the specification and migration of longitudinal gut muscle founders from the caudal mesoderm of Drosophila. *Development* **137**, 3107-3117.

Izumi, Y., Yanagihashi, Y. and Furuse, M. (2012). A novel protein complex, Mesh-Ssk, is required for septate junction formation in the Drosophila midgut. *J. Cell Sci.* **125**, 4923-4933.

Kelly, R. G. (2012). The second heart field. *Curr. Top. Dev. Biol.* **100**, 33-65.

LaBeau, E. M., Trujillo, D. L. and Cripps, R. M. (2009). Bithorax complex genes control alary muscle patterning along the cardiac tube of Drosophila. *Mech. Dev.* **126**, 478-486.

Laugwitz, K.-L., Moretti, A., Lam, J., Gruber, P., Chen, Y., Woodard, S., Lin, L.-Z., Cai, C.-L., Lu, M. M., Reth, M. et al. (2005). Postnatal isl1+ cardioblasts enter fully differentiated cardiomyocyte lineages. *Nature* **433**, 647-653.

Lehmacher, C., Abeln, B. and Paululat, A. (2012). The ultrastructure of Drosophila heart cells. *Arthropod Struct. Dev.* **41**, 459-474.

Mann, T., Bodmer, R. and Pandur, P. (2009). The Drosophila homolog of vertebrate Islet1 is a key component in early cardiogenesis. *Development* **136**, 317-326.

Markstein, M., Pitsouli, C., Villalta, C., Celniker, S. E. and Perrimon, N. (2008). Exploiting position effects and the gypsy retrovirus insulator to engineer precisely expressed transgenes. *Nat. Genet.* **40**, 476-483.

Merrell, A. J. and Kardon, G. (2013). Development of the diaphragm – a skeletal muscle essential for mammalian respiration. *FEBS J.* **280**, 4026-4035.

Moretti, A., Caron, L., Nakano, A., Lam, J. T., Bernshausen, A., Chen, Y., Qyang, Y., Bu, L., Sasaki, M., Martin-Puig, S. et al. (2006). Multipotent embryonic isl1+ progenitor cells lead to cardiac, smooth muscle, and endothelial cell diversification. *Cell* **127**, 1151-1165.

Müller, C. W. and Herrmann, B. G. (1997). Crystallographic structure of the T domain-DNA complex of the Brachyury transcription factor. *Nature* **389**, 884-888.

Nose, A., Isshiki, T. and Takeichi, M. (1998). Regional specification of muscle progenitors in Drosophila: the role of the msh homeobox gene. *Development* **125**, 215-223.

Okumura, T., Fujiwara, H., Taniguchi, K., Kuroda, J., Nakazawa, N., Nakamura, M., Hatori, R., Ishio, A., Maeda, R. and Matsuno, K. (2010). Left-right asymmetric morphogenesis of the anterior midgut depends on the activation of a non-muscle myosin II in Drosophila. *Dev. Biol.* **344**, 693-706.

Portales-Casamar, E., Thongjuea, S., Kwon, A. T., Arenillas, D., Zhao, X., Valen, E., Yusuf, D., Lenhard, B., Wasserman, W. W. and Sandelin, A. (2010). JASPAR 2010: the greatly expanded open-access database of transcription factor binding profiles. *Nucleic Acids Res.* **38**, D105-D110.

Prall, O. W. J., Menon, M. K., Solloway, M. J., Watanabe, Y., Zaffran, S., Bajolle, F., Biben, C., McBride, J. J., Robertson, B. R., Chaulet, H. et al. (2007). An

Nkx2-5/Bmp2/Smad1 negative feedback loop controls heart progenitor specification and proliferation. *Cell* **128**, 947-959.

Razy-Krajka, F., Lam, K., Wang, W., Stolfi, A., Joly, M., Bonneau, R. and Christiaen, L. (2014). Collier/OLF/EBF-dependent transcriptional dynamics control pharyngeal muscle specification from primed cardiopharyngeal progenitors. *Dev. Cell* **29**, 263-276.

Rizki, T. M. (1978). The circulatory system and associated cells and tissues. In *The Genetics and Biology of Drosophila* (ed. M. Ashburner and T. R. F. Wright), pp. 397-452. New York: Academic Press.

Rushton, E., Drysdale, R., Abmayr, S. M., Michelson, A. M. and Bate, M. (1995). Mutations in a novel gene, myoblast city, provide evidence in support of the founder cell hypothesis for Drosophila muscle development. *Development* **121**, 1979-1988.

Sambasivan, R., Gayraud-Morel, B., Dumas, G., Cimper, C., Paisant, S., Kelly, R. G. and Tajbakhsh, S. (2009). Distinct regulatory cascades govern extraocular and pharyngeal arch muscle progenitor cell fates. *Dev. Cell* **16**, 810-821.

Sandmann, T., Girardot, C., Brehme, M., Tongprasit, W., Stolc, V. and Furlong, E. E. M. (2007). A core transcriptional network for early mesoderm development in Drosophila melanogaster. *Genes Dev.* **21**, 436-449.

Schaub, C. and Frasch, M. (2013). Org-1 is required for the diversification of circular visceral muscle founder cells and normal midgut morphogenesis. *Dev. Biol.* **376**, 245-259.

Schaub, C., Nagaso, H., Jin, H. and Frasch, M. (2012). Org-1, the Drosophila ortholog of Tbx1, is a direct activator of known identity genes during muscle specification. *Development* **139**, 1001-1012.

Sellin, J., Drechsler, M., Nguyen, H. T. and Paululat, A. (2009). Antagonistic function of Lmd and Zfh1 fine tunes cell fate decisions in the Twi and Tin positive mesoderm of Drosophila melanogaster. *Dev. Biol.* **326**, 444-455.

Sosinsky, A., Bonin, C. P., Mann, R. S. and Honig, B. (2003). Target Explorer: an automated tool for the identification of new target genes for a specified set of transcription factors. *Nucleic Acids Res.* **31**, 3589-3592.

Sudarsan, V., Pasalodos-Sanchez, S., Wan, S., Gampel, A. and Skaer, H. (2002). A genetic hierarchy establishes mitogenic signalling and mitotic competence in the renal tubules of Drosophila. *Development* **129**, 935-944.

Tao, Y., Wang, J., Tokusumi, T., Gajewski, K. and Schulz, R. A. (2007). Requirement of the LIM homeodomain transcription factor Tailup for normal heart and hematopoietic organ formation in Drosophila melanogaster. *Mol. Cell. Biol.* **27**, 3962-3969.

Thor, S. and Thomas, J. B. (1997). The Drosophila islet gene governs axon pathfinding and neurotransmitter identity. *Neuron* **18**, 397-409.

Tiklová, K., Tsarouhas, V. and Samakovlis, C. (2013). Control of airway tube diameter and integrity by secreted chitin-binding proteins in Drosophila. *PLoS ONE* **8**, e67415.

Vincent, S. D. and Buckingham, M. E. (2010). How to make a heart: the origin and regulation of cardiac progenitor cells. *Curr. Top. Dev. Biol.* **90**, 1-41.

Wang, W., Razy-Krajka, F., Siu, E., Ketcham, A. and Christiaen, L. (2013). NK4 antagonizes Tbx1/10 to promote cardiac versus pharyngeal muscle fate in the ascidian second heart field. *PLoS Biol.* **11**, e1001725.

Watanabe, Y., Zaffran, S., Kuroiwa, A., Higuchi, H., Ogura, T., Harvey, R. P., Kelly, R. G. and Buckingham, M. (2012). Fibroblast growth factor 10 gene regulation in the second heart field by Tbx1, Nkx2-5, and Islet1 reveals a genetic switch for down-regulation in the myocardium. *Proc. Natl. Acad. Sci. USA* **109**, 18273-18280.

Weavers, H. and Skaer, H. (2013). Tip cells act as dynamic cellular anchors in the morphogenesis of looped renal tubules in Drosophila. *Dev. Cell* **27**, 331-344.

Zaffran, S., Reim, I., Qian, L., Lo, P. C., Bodmer, R. and Frasch, M. (2006). Cardioblast-intrinsic Tinman activity controls proper diversification and differentiation of myocardial cells in Drosophila. *Development* **133**, 4073-4083.

Zinzen, R. P., Girardot, C., Gagneur, J., Braun, M. and Furlong, E. E. M. (2009). Combinatorial binding predicts spatio-temporal cis-regulatory activity. *Nature* **462**, 65-70.

Zmojdzian, M., Da Ponte, J. P. and Jagla, K. (2008). Cellular components and signals required for the cardiac outflow tract assembly in Drosophila. *Proc. Natl. Acad. Sci. USA* **105**, 2475-2480.

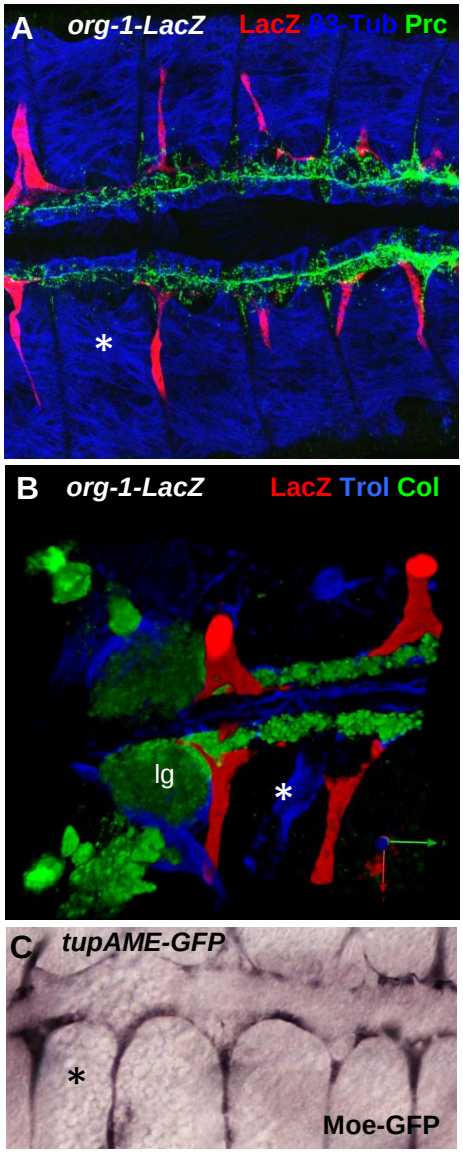

Fgure S1: Connection of alary muscles to pericardial cells and the lymph gland.

(A, B) dorsal views stage 16 *org-1-lacZ* embryo stained for β-gal (red) and (A) Prc (green) and β3-Tub (blue) and (B), Trol (blue) and Col (green), showing the connection of alary fibers to the ECM surrounding the dorsal vessel (A) and (B), the posterior part of the lymph gland (lg). (B) is a 3D reconstruction of a dorsal view. (C) Staining of *tupAME-moeGFP* embryo for GFP shows that the dorsal aliform extensions of adjacent AMs are connected dorsally. The asterisk indicates the A2 segment.

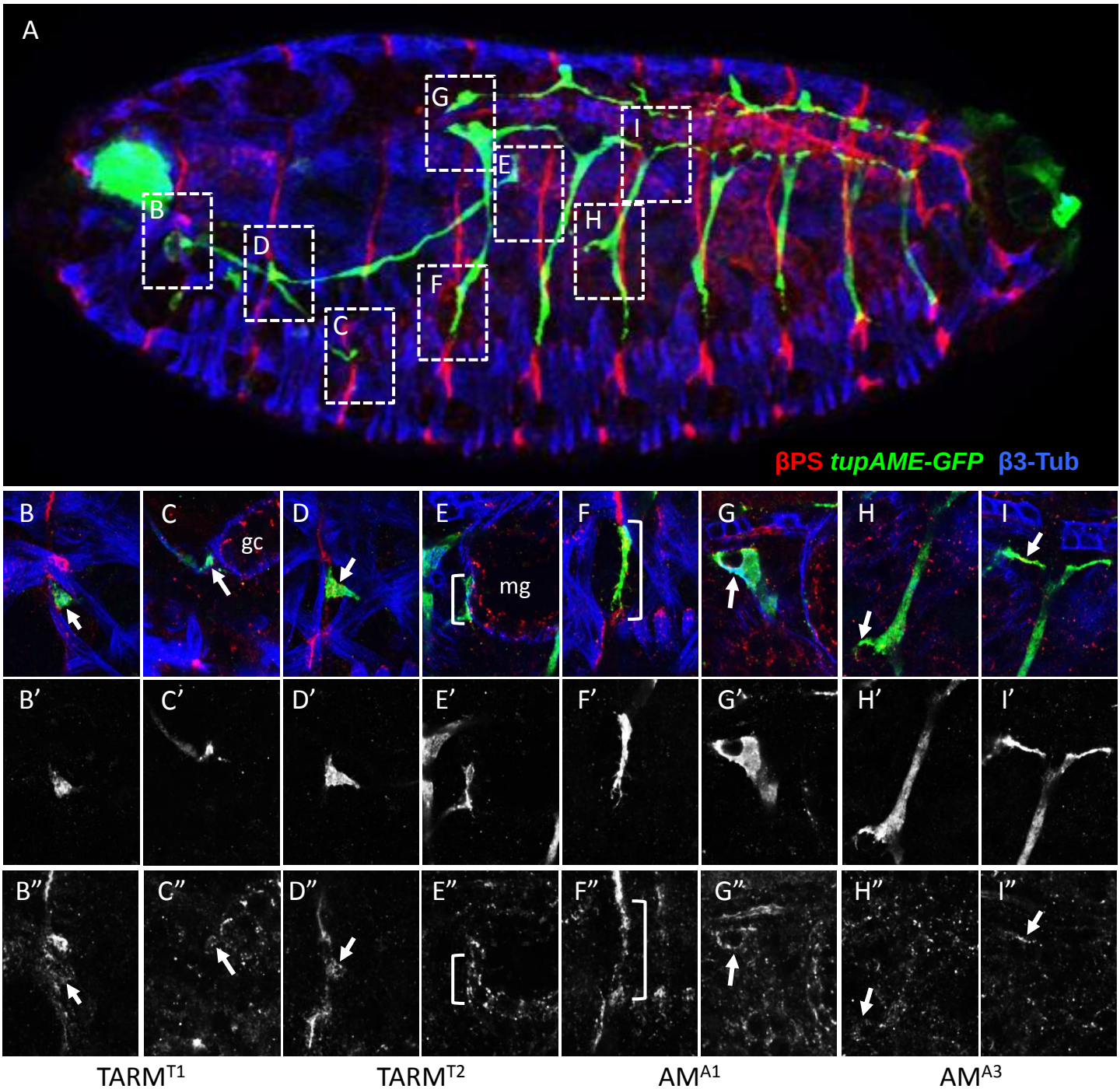

Figure S2. Integrin-mediated attachment of AMs and TARMs.

Stage 16 *tupAME-moeGFP* embryo stained for GFP (green), β3-Tub (blue) and βPS integrin (red) to visualize AMs and TARMs, somatic and visceral muscles and integrin accumulation sites, respectively. (A) Whole embryo; B-I'', enlarged views of AMs/TARMs attachment sites (according to lettered frames in A); overlay (B-I), green (B'-I') and red channel alone (B"-I") are shown. (B, C) $TARM^{T1}$ – epidermal (B) and (C) gastric caeca (gc) attachment. (D, E) $TARM^{T2}$ epidermal (D), and, (E) midgut (mg) attachment. (F, G) AM^{A1} epidermal (F) and (G) lymph gland attachment. (H,I) AM^{A3} MT tip cell (H) and (I) heart attachment. Note the multiple cytoplasmic extensions at the tips of AMs and TARMs. βPS integrin accumulation is observed at all AM/TARM attachment sites (arrows).

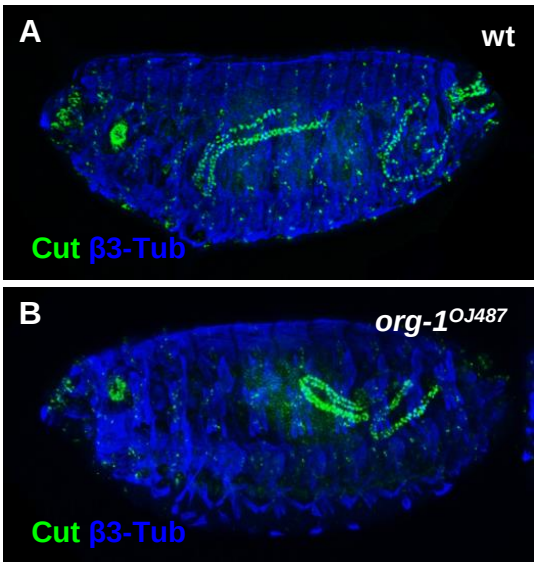

Figure S3: Malpighian Tubules fail to elongate properly in *org-1* mutant embryos.

Cut and β-3 tubulin staining of wt (A) and *org-1*^{OJ487} (B) stage 16 embryos shows the abnormal positioning of MTs in absence of *org-1* function.

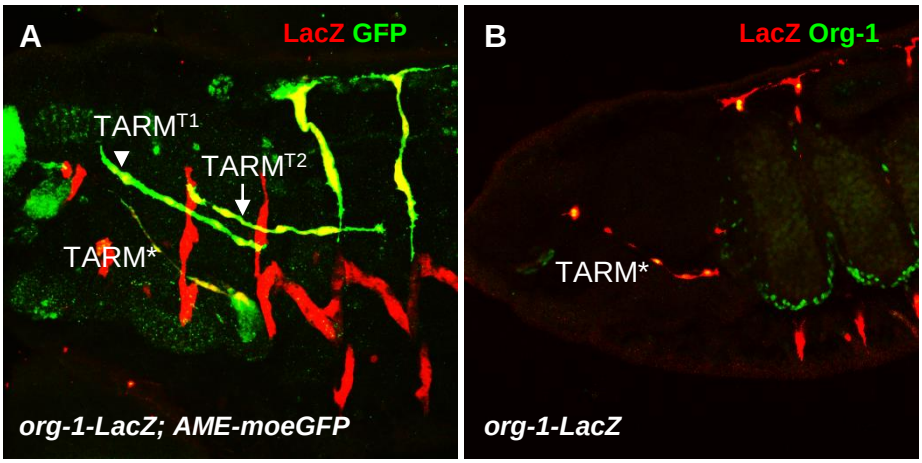

Figure S4: TARM*, a third alary-related muscle in the thoracic region

(A) Lateral views of stage 16 *org-1-lacZ; tupAME-moeGFP* embryo stained with β-gal (red) and GFP (green) reveals an additional Org+ Tup+ fiber in the thoracic region. (B) Lateral view of stage 16 *org-1-lacZ* embryo stained with β-gal (red) and Org-1 (green). A z stack shows that TARM* is a thin and multinucleated fiber.

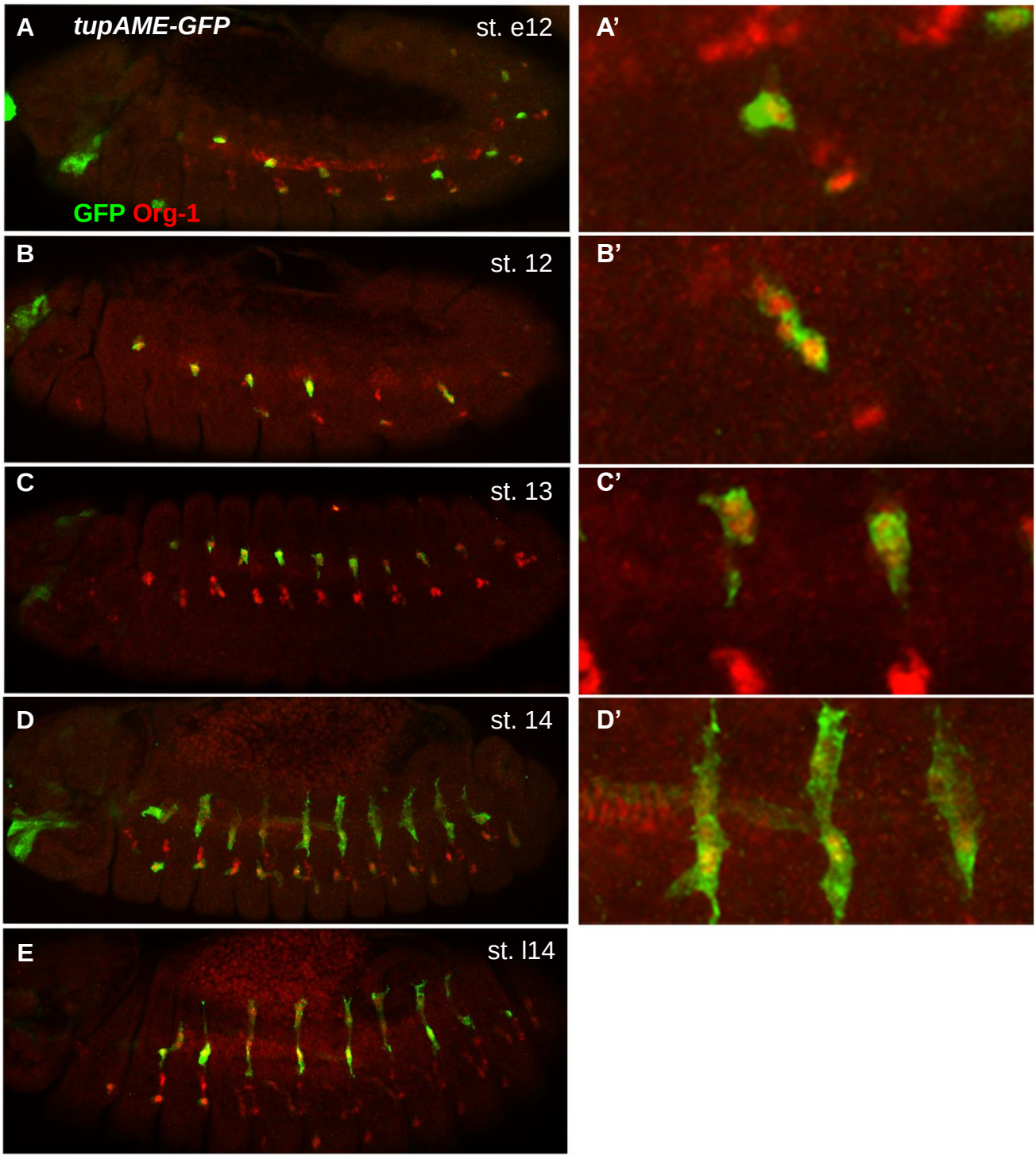

Figure S5. Stepwise development of AMs.

(A-E**)** Lateral views of *tupAME-moeGFP* embryos stained for GFP (green) and Org-1 (red). Developmental stages are indicated on each panel. (A'-D') close up views.

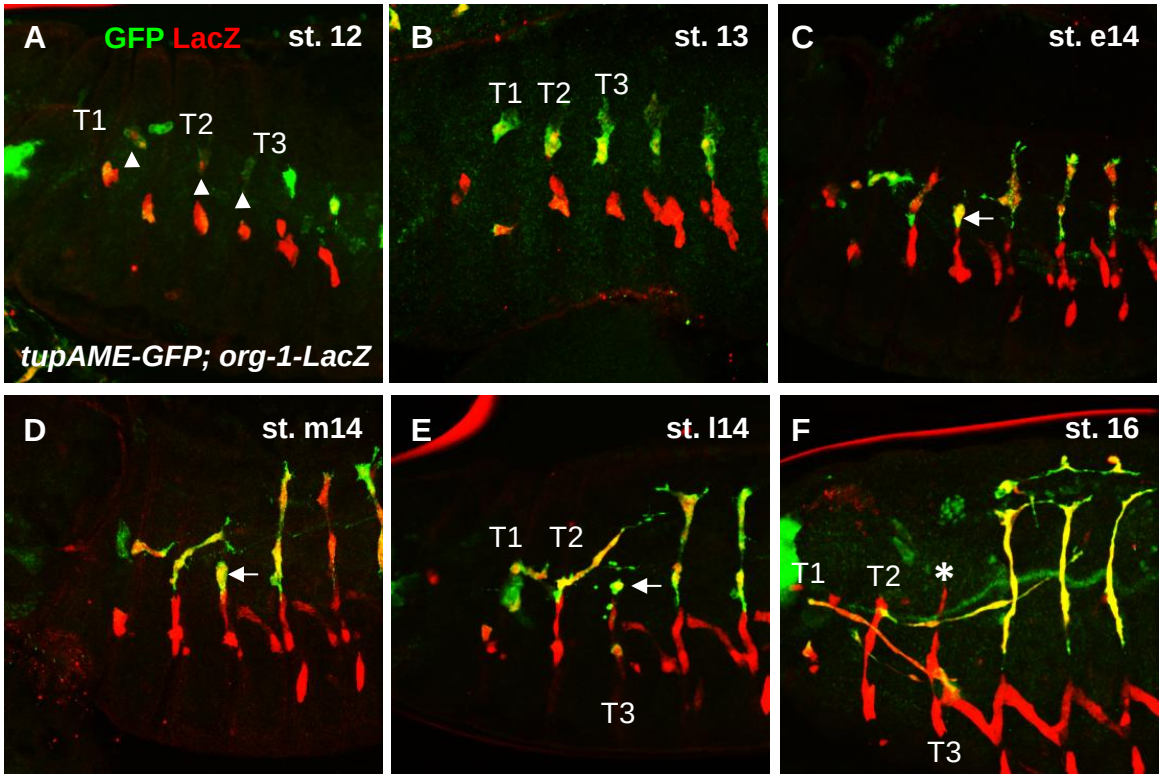

Figure S6. Stepwise development of TARMs

(A-F) Lateral views of *tupAME-moeGFP; org-1-lacZ* embryos stained for GFP (green) and β-gal (red); only the T1, T2, and T3 segments are shown. Developmental stages are indicated on each panel. The *tup/org-1* positive AM progenitors are indicated by arrowheads in A. Development of $TARM^{T3}$ proceeds similar to $TARM^{T1}$ and $TARM^{T2}$ until stage 14, when it stops to elongate (arrows in C-E). (F) No *org-1-lacZ*/*tup-GFP* cell is detected in T3 at stage 16 (white asterisk).

Figure S7. *D. melanogaster*_FlyBase positions (release: r5.42) 2L: 18899345..18900688. Conserved sequence blocks between *D. melanogaster*, *D.sechellia*, *D.simulans*, *D.yakuba*, *D.erecta*, *D.pseudoobscura*, *D.persimilis*, *D.ananassae*, *D.willistoni* and *D.virilis* are indicated by bold capital letters. The position of predicted binding sites for Org-1, Mef-2, Tup and Twist are color-coded as indicated in the margin. The position of the AME fragment is underlined in red. The limit between the ADME.II and AME.I fragments is indicated by :

Supplementary Movie 1: Time-lapse recording of alary muscle development.
Embryos expressing *tupF4*-GFP and *org-1*-RFP in developing alary muscles and subsets of somatic muscles and AMPs as described in the text were imaged over the time course of 9 hours from stages early 12 to 17 (lateral view). *tupF4*-GFP preferentially localizes to nuclei and also labels all heart cells. *tupF4*-GPF is already detectable in the AM progenitor cell at the beginning of the movie, while detectability of fluorescence from *org-1*-RFP in AMs is delayed as compared to endogenous Org-1 expression. Co-expression of GFP and RFP is clearly detectable in AM and TARM fibers. Due to some ectopic activity of the *tupF4* enhancer co-localization also occurs in the LO1/VT1 PC, located ventrally to the AM PC, and its derived muscles.

Movie 1.